Chapter 3

Cahn-Hilliard Equation with degenerate mobility

In chapter 2, we considered the constant mobility case in Cahn-Hilliard equation, but the original derivation of the equation a concentration dependent mobility appeared [32]. Therefore, in this chapter, we consider an efficient and accurate finite difference multigrid approximation of the Cahn-Hilliard equation with degenerate mobility

$$\frac{\partial c}{\partial t} = \nabla \cdot (M(c)\nabla \mu(c)), \quad x \in \Omega, \ t > 0, \tag{3.0.1}$$

$$\mu(c) = F'(c) - \epsilon^2 \Delta c. \tag{3.0.2}$$

This equation arises from the Ginzburg-Landau free energy

$$\mathcal{E}(c) := \int_\Omega \left(F(c) + \frac{\epsilon^2}{2} |\nabla c|^2 \right) dx.$$

$F(c)$ is the Helmholtz free energy and $\frac{\epsilon^2}{2}|\nabla c|^2$ penalizes the occurrence of interfaces where c changes rapidly and thus models the influence of the interfacial energy. To obtain the Cahn-Hilliard equation with degenerate mobility one introduces a chemical potential μ as the variational derivative of $\mathcal{E}$,

$$\mu := \frac{\delta \mathcal{E}}{\delta c} = F'(c) - \epsilon^2 \Delta c,$$

and defines the flux,

$$\mathcal{J} := -M(c)\nabla \mu,$$

where $M(c) \geq 0$ is a diffusional mobility. We took a mobility of the form $M(c) := c(1-c)$, which is a thermodynamically reasonable choice [43]. This mobility significantly lowers the long-range diffusion across bulk regions. This is particularly appropriate when we study fluid flows with immiscible components. Our development here is in preparation for such studies presented in the later chapters of this thesis.

Having defined the flux the Cahn-Hilliard with degenerate mobility now follows from the equation

$$\frac{\partial c}{\partial t} = -\nabla \cdot \mathcal{J},$$

which is a consequence of mass conservation. The system is completed by taking initial conditions and the natural and no-flux boundary conditions

$$\frac{\partial c}{\partial n} = \mathcal{J} \cdot n = 0 \text{ on } \partial\Omega, \tag{3.0.3}$$

where n is normal to $\partial\Omega$. We differentiate the energy $\mathcal{E}$ and use the boundary condition (3.0.3) to get

$$\begin{aligned}
\frac{d}{dt}\mathcal{E}(t) &= \frac{d}{dt}\int_\Omega \left(F(c) + \frac{\epsilon^2}{2}|\nabla c|^2 \right) dx \\
&= \int_\Omega (F'(c)c_t + \epsilon^2 \nabla c \cdot \nabla c_t) dx = \int_\Omega \mu c_t dx = \int_\Omega \mu \nabla \cdot (M(c)\nabla\mu) dx \\
&= \int_{\partial\Omega} \mu M(c) \frac{\partial \mu}{\partial n} ds - \int_\Omega \nabla\mu \cdot (M(c)\nabla\mu) dx = -\int_\Omega M(c)|\nabla\mu|^2 dx
\end{aligned}$$

Therefore, the total energy is non-increasing in time.

3.1 The Scheme

We present a semi-implicit time (Crank-Nicholson) and centered difference space discretizations of equations (3.0.1) and (3.0.2).

$$\frac{c_{ij}^{n+1} - c_{ij}^n}{\Delta t} = \frac{1}{\mathbf{Pe}} \tilde{\nabla}_d^e \cdot [M(c_{ij}^{n+\frac{1}{2}}) \nabla_d^e \mu_{ij}^{n+\frac{1}{2}}] + s_{ij}^{n+\frac{1}{2}}, \tag{3.1.4}$$

$$\mu_{ij}^{n+\frac{1}{2}} = \frac{1}{2}(f(c_{ij}^{n+1}) + f(c_{ij}^n)) - \frac{\epsilon^2}{2}(\Delta_d c_{ij}^{n+1} + \Delta_d c_{ij}^n). \tag{3.1.5}$$

where $f(c) = F'(c)$ and $s_{ij}^{n+\frac{1}{2}}$ is a source term due to advection, for example. Mass conservation and stability estimate of a discrete energy functional are established in the following theorem.

Theorem 3.1. *If $\{c^n, \mu^{n+\frac{1}{2}}\}$ is the solution of (3.1.4) and (3.1.5) with $s_{ij}^{n+\frac{1}{2}} = 0$ and if we define the discrete energy functional by*

$$\mathcal{E}_h(c^n) = (F(c^n), 1)_h + \frac{\epsilon^2}{2}|c^n|_{e,1}^2,$$

for simplicity, let $\mathbf{Pe} = 1$, then

$$(c^{n+1}, 1)_h = (c^n, 1)_h.$$

$$\mathcal{E}_h(c^{n+1}) - \mathcal{E}_h(c^n) \leq -(\Delta t - \frac{C(\Delta t)^2}{h^2})(M\nabla_d^e \mu^{n+\frac{1}{2}}, \nabla_d^e \mu^{n+\frac{1}{2}})_e.$$

Proof.

$$\begin{aligned}(c^{n+1}, 1)_h &= (c^n, 1)_h + \Delta t(\tilde{\nabla}_d^e \cdot (M\nabla_d^e \mu^{n+\frac{1}{2}}), 1)_h \\ &= (c^n, 1)_h - \Delta t(M\nabla_d^e \mu^{n+\frac{1}{2}}, \nabla_d^e 1)_e = (c^n, 1)_h.\end{aligned}$$

It remains to prove the second assertion. Multiplying $\mu^{n+\frac{1}{2}}$ and $c^{n+1} - c^n$ to (3.1.4) and (3.1.5), respectively and summing by parts, we obtain the following two identities

$$(c^{n+1} - c^n, \mu^{n+\frac{1}{2}})_h + \Delta t(M\nabla_d^e \mu^{n+\frac{1}{2}}, \nabla_d^e \mu^{n+\frac{1}{2}})_e = 0,$$

$$\begin{aligned}(c^{n+1} - c^n, \mu^{n+\frac{1}{2}})_h &= \frac{1}{2}(c^{n+1} - c^n, f(c^{n+1}) + f(c^n))_h - \frac{\epsilon^2}{2}(c^{n+1} - c^n, \Delta_d c^{n+1} + \Delta_d c^n)_h \\ &= \frac{1}{2}(c^{n+1} - c^n, f(c^{n+1}) + f(c^n))_h + \frac{\epsilon^2}{2}(|c^{n+1}|_{e,1} - |c^n|_{e,1})\end{aligned}$$

Next, using our scheme (3.1.4) and (3.1.5), we also have the following estimates.

$$||c^{n+1} - c^n||^2 \leq \frac{C|\Delta t|^2}{h^2}||M\nabla_d^e \mu^{n+\frac{1}{2}}||^2,$$

$$|c^{n+1} - c^n|_{e,1}^2 \leq \frac{C|\Delta t|^2}{h^4}|\mu^{n+\frac{1}{2}}|_{e,1}^2,$$

where C depends on the dimension of domain of Ω.

Indeed, multiplying $c^{n+1} - c^n$ to (3.1.4) and the Hölder inequality, we obtain

$$||c^{n+1} - c^n||^2 \leq \Delta t||M\nabla_d^e \mu^{n+\frac{1}{2}}|||c^{n+1} - c^n|_{e,1}$$

On the other hand, the following inequality can be easily verified

$$|c^{n+1} - c^n|_{e,1}^2 \leq \frac{C}{h^2}||c^{n+1} - c^n||^2,$$

Combining the above inequalities, we get

$$||c^{n+1} - c^n|| \leq \frac{C\Delta t}{h}||M\nabla_d^e \mu^{n+\frac{1}{2}}||.$$

The second estimate is easy consequence of first one. Indeed,

$$|c^{n+1} - c^n|_{e,1}^2 \leq \frac{C}{h^2}||c^{n+1} - c^n||^2 \leq \frac{C|\Delta t|^2}{h^4}||M\nabla_d^e \mu^{n+\frac{1}{2}}||^2.$$

Using the identities above, we obtain

$$\begin{aligned}\mathcal{E}_h(c^{n+1}) - \mathcal{E}_h(c^n) &= (F(c^{n+1}) - F(c^n), 1)_h + \tfrac{\epsilon^2}{2}|c^{n+1}|_{e,1}^2 - \tfrac{\epsilon^2}{2}|c^n|_{e,1}^2 \\ &= (F(c^{n+1}) - F(c^n), 1)_h - \Delta t(M\nabla_d^e \mu^{n+\frac{1}{2}}, \nabla_d^e \mu^{n+\frac{1}{2}})_e \\ &\quad -\tfrac{1}{2}(f(c^{n+1}) + f(c^n), c^{n+1} - c^n)_h\end{aligned}$$

Since F is differentiable, the first term in right side is estimated as follows:

$$F(c^{n+1}) - F(c^n) = f(\frac{c^{n+1}+c^n}{2})(c^{n+1}-c^n) + O((c^{n+1}-c^n)^2).$$

Therefore,

$$\begin{aligned}
\mathcal{E}_h(c^{n+1}) - \mathcal{E}_h(c^n) &\le \left(\frac{F(c^{n+1})-F(c^n)}{c^{n+1}-c^n} - \frac{1}{2}(f(c^{n+1})+f(c^n)), c^{n+1}-c^n\right)_h \\
&\quad -\Delta t(M\nabla_d^e \mu^{n+\frac{1}{2}}, \nabla_d^e \mu^{n+\frac{1}{2}})_e \\
&= \left(f(\frac{c^{n+1}+c^n}{2}) - \frac{1}{2}(f(c^{n+1})+f(c^n)) + O(c^{n+1}-c^n), c^{n+1}-c^n\right)_h \\
&\quad -\Delta t(M\nabla_d^e \mu^{n+\frac{1}{2}}, \nabla_d^e \mu^{n+\frac{1}{2}})_e \\
&= \big(O((c^{n+1}-c^n)^2) + O(c^{n+1}-c^n), c^{n+1}-c^n\big)_h \\
&\quad -\Delta t(M\nabla_d^e \mu^{n+\frac{1}{2}}, \nabla_d^e \mu^{n+\frac{1}{2}})_e \\
&\le C\|c^{n+1}-c^n\|^2 - \Delta t(M\nabla_d^e \mu^{n+\frac{1}{2}}, \nabla_d^e \mu^{n+\frac{1}{2}})_e \\
&\le \frac{C\Delta t^2}{h^2}\|M\nabla_d^e \mu^{n+\frac{1}{2}}\|^2 - \Delta t(M\nabla_d^e \mu^{n+\frac{1}{2}}, \nabla_d^e \mu^{n+\frac{1}{2}})_e \\
&\le \frac{C\Delta t^2}{h^2}(M\nabla_d^e \mu^{n+\frac{1}{2}}, \nabla_d^e \mu^{n+\frac{1}{2}})_e - \Delta t(M\nabla_d^e \mu^{n+\frac{1}{2}}, \nabla_d^e \mu^{n+\frac{1}{2}})_e \\
&= (\frac{C\Delta t^2}{h^2} - \Delta t)(M\nabla_d^e \mu^{n+\frac{1}{2}}, \nabla_d^e \mu^{n+\frac{1}{2}})_e
\end{aligned}$$

This completes the theorem. □

3.2 Solution of implicit discretization

In this section, the solution of the implicit discrete Cahn-Hilliard system with degenerate mobility and a source term is presented using a nonlinear multigrid method. Let us rewrite equations (3.1.4), (3.1.5) as follows.

$$\mathbf{NSO}(c^{n+1}, \mu^{n+\frac{1}{2}}) = (f^n, g^n),$$

where

$$\mathbf{NSO}(c^{n+1}, \mu^{n+\frac{1}{2}}) = (\frac{c_{ij}^{n+1}}{\Delta t} - \tilde{\nabla}_d^e \cdot [M(c_{ij})^{n+\frac{1}{2}} \nabla_d^e \mu_{ij}^{n+\frac{1}{2}}], \mu_{ij}^{n+\frac{1}{2}} - \frac{1}{2} f(c_{ij}^{n+1}) + \frac{\epsilon^2}{2}\Delta_d c_{ij}^{n+1}),$$

and the source term is

$$(f^n,\ g^n) = (\frac{c_{ij}^n}{\Delta t} + s_{ij}^{n+\frac{1}{2}},\ \frac{1}{2} f(c_{ij}^n) - \frac{\epsilon^2}{2}\Delta_d c_{ij}^n).$$

Here, we derive the smoothing operator in two dimensions (the corresponding operator in 3-D is presented in chapter 5). Recall that the scheme is

$$\begin{aligned}\frac{c_{ij}^{n+1}-c_{ij}^{n}}{\Delta t} &= \frac{1}{\mathbf{Pe}}\tilde{\nabla}_d^e\cdot[M(c_{ij}^{n+\frac{1}{2}})\nabla_d^e\mu_{ij}^{n+\frac{1}{2}}]+s_{ij}^{n+\frac{1}{2}},\\ \mu_{ij}^{n+\frac{1}{2}} &= \frac{1}{2}(f(c_{ij}^{n+1})+f(c_{ij}^{n}))-\frac{\epsilon^2}{2}(\Delta_d c_{ij}^{n+1}+\Delta_d c_{ij}^{n}).\end{aligned}$$

Rewriting these equations, we get

$$\begin{aligned}\frac{c_{ij}^{n+1}}{\Delta t} &+ \left[\frac{M(c_{i+\frac{1}{2},j}^{n+\frac{1}{2}})+M(c_{i-\frac{1}{2},j}^{n+\frac{1}{2}})}{\mathbf{Pe}\Delta x^2}+\frac{M(c_{i,j+\frac{1}{2}}^{n+\frac{1}{2}})+M(c_{i,j-\frac{1}{2}}^{n+\frac{1}{2}})}{\mathbf{Pe}\Delta y^2}\right]\mu_{ij}^{n+\frac{1}{2}}\\ &= \frac{c_{ij}^{n}}{\Delta t}+s_{ij}^{n+\frac{1}{2}}+\frac{M(c_{i+\frac{1}{2},j}^{n+\frac{1}{2}})\mu_{i+1,j}^{n+\frac{1}{2}}+M(c_{i-\frac{1}{2},j}^{n+\frac{1}{2}})\mu_{i-1,j}^{n+\frac{1}{2}}}{\mathbf{Pe}\Delta x^2}\\ &\quad+\frac{M(c_{i,j+\frac{1}{2}}^{n+\frac{1}{2}})\mu_{i,j+1}^{n+\frac{1}{2}}+M(c_{i,j-\frac{1}{2}}^{n+\frac{1}{2}})\mu_{i,j-1}^{n+\frac{1}{2}}}{\mathbf{Pe}\Delta y^2},\end{aligned} \tag{3.2.6}$$

where $M(c_{i+\frac{1}{2},j}^{n+\frac{1}{2}})=[M((c_{ij}^{n+1}+c_{i+1,j}^{n+1})/2)+M((c_{ij}^{n}+c_{i+1,j}^{n})/2)]/2$ and the other values, $M(c_{i-\frac{1}{2},j}^{n+\frac{1}{2}})$, $M(c_{i,j+\frac{1}{2}}^{n+\frac{1}{2}})$, and $M(c_{i,j-\frac{1}{2}}^{n+\frac{1}{2}})$ are calculated similarly.

$$\begin{aligned}-[\frac{\epsilon^2}{\Delta x^2}+\frac{\epsilon^2}{\Delta y^2}]c_{ij}^{n+1}+\mu_{ij}^{n+\frac{1}{2}} &= \frac{1}{2}f(c_{ij}^{n+1})+\frac{1}{2}f(c_{ij}^{n})-\frac{\epsilon^2}{2}\Delta_d c_{ij}^{n}\\ &\quad-\frac{\epsilon^2}{2\Delta x^2}(c_{i+1,j}^{n+1}+c_{i-1,j}^{n+1})-\frac{\epsilon^2}{2\Delta y^2}(c_{i,j+1}^{n+1}+c_{i,j-1}^{n+1}).\end{aligned} \tag{3.2.7}$$

Next, linearize the term in above equation containing $f(c_{ij}^{n+1})$, i.e.

$$f(c_{ij}^{n+1})\approx f(c_{ij}^{m})+\frac{df}{dc}(c_{ij}^{m})(c_{ij}^{n+1}-c_{ij}^{m}).$$

After substitution of this into (3.2.7), we get

$$\begin{aligned}-[\frac{\epsilon^2}{\Delta x^2}+\frac{\epsilon^2}{\Delta y^2}+\frac{1}{2}\frac{df}{dc}(c_{ij}^{m})]c_{ij}^{n+1}+\mu_{ij}^{n+\frac{1}{2}} &= \frac{1}{2}f(c_{ij}^{n})-\frac{\epsilon^2}{2}\Delta_d c_{ij}^{n}+\frac{1}{2}f(c_{ij}^{m})-\frac{1}{2}\frac{df}{dc}(c_{ij}^{m})c_{ij}^{m}\\ &\quad-\frac{\epsilon^2}{2\Delta x^2}(c_{i+1,j}^{m+1}+c_{i-1,j}^{m+1})-\frac{\epsilon^2}{2\Delta y^2}(c_{i,j+1}^{m+1}+c_{i,j-1}^{m+1}).\end{aligned} \tag{3.2.8}$$

The smoother then consists of solving the 2×2 system (3.2.6) and (3.2.8) for c_{ij}^{n+1} and $\mu_{ij}^{n+\frac{1}{2}}$. With these **NSO** and a smooth operator, we apply the same nonlinear multigrid procedure which is described in chapter 2.

3.3 Numerical experiments

In this section, we demonstrate in the case of a degenerate mobility a quite different qualitative behavior is observed when compared to results obtained with constant mobility. In the paper [82], finite element approximation is used to solve the (**C-H**) equation with degenerate mobility numerically and we take similar a test problem in there. We performed two numerical experiments in two spatial dimensions with $\Omega = (0,1) \times (0,1)$ and $s_{ij}^{n+\frac{1}{2}} = 0$. In the first experiment we took the degenerate mobility, $M(c) := c(1-c)$. In the second experiment we took exactly the same data, but with constant mobility, $M(c) \equiv 1$.

The initial data were taken to be $c^0 = 0.25 + 0.2\cos(2\pi \text{ rand()})$, where rand() is a random number between 0 and 1. $\epsilon = 0.004,\ \Delta t = 0.1/128,$ and mesh size 128×128. We stop the numerical computations when the error between $(m+1)^{th}-$ and $m^{th}-$ iterations become less than 10^{-7}. That is $\|c^{m+1} - c^m\| \leq 10^{-7}$. The pictures are arranged in a matrix format with time increasing to the right in rows then down columns. The final numerical solution plotted in Fig. 3.1 is a stationary numerical solution according to the stopping criteria.

In Fig. 3.1, the case of degenerate mobility, second-phase regions are nucleated (black regions). The surface energy in the **C-H** system causes the regions to be circular. There is evidence of a small amount of coarsening as small regions vanish and redistribute their mass to the other regions. There seems to be a minimum radius for viability of the region. As the remaining regions grow, an equilibrium is established when the two-phase domain is nearly monodisperse. The degenerate mobility generally reduces diffusion in the bulk. This is made clear by comparing to the results in Fig. 3.2 where the mobility is constant. For this case, the initial data is taken to be $c^0 \equiv c(\cdot, 23.92)$ from the first experiment. In the case of constant mobility, the evolution leads to a microstructure consisting entirely of a single large, semi-circular second-phase domains.

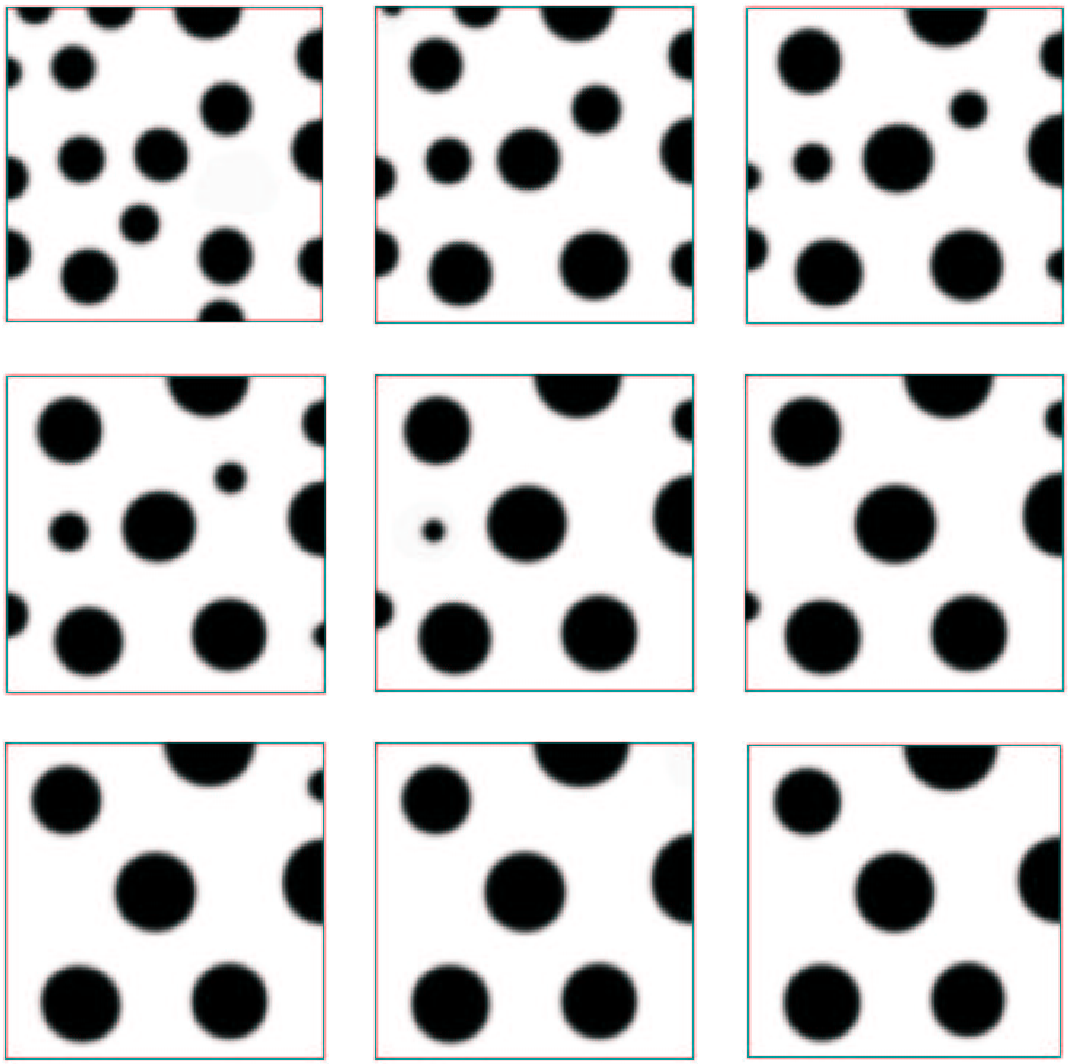

Figure 3.1: $c(\cdot,t)$ plotted for $t = 23.92, 55.80, 91.68, 99.65, 119.58, 131.54, 139.51, 151.47,$ and 195.31 when $M(c) := c(1-c)$.

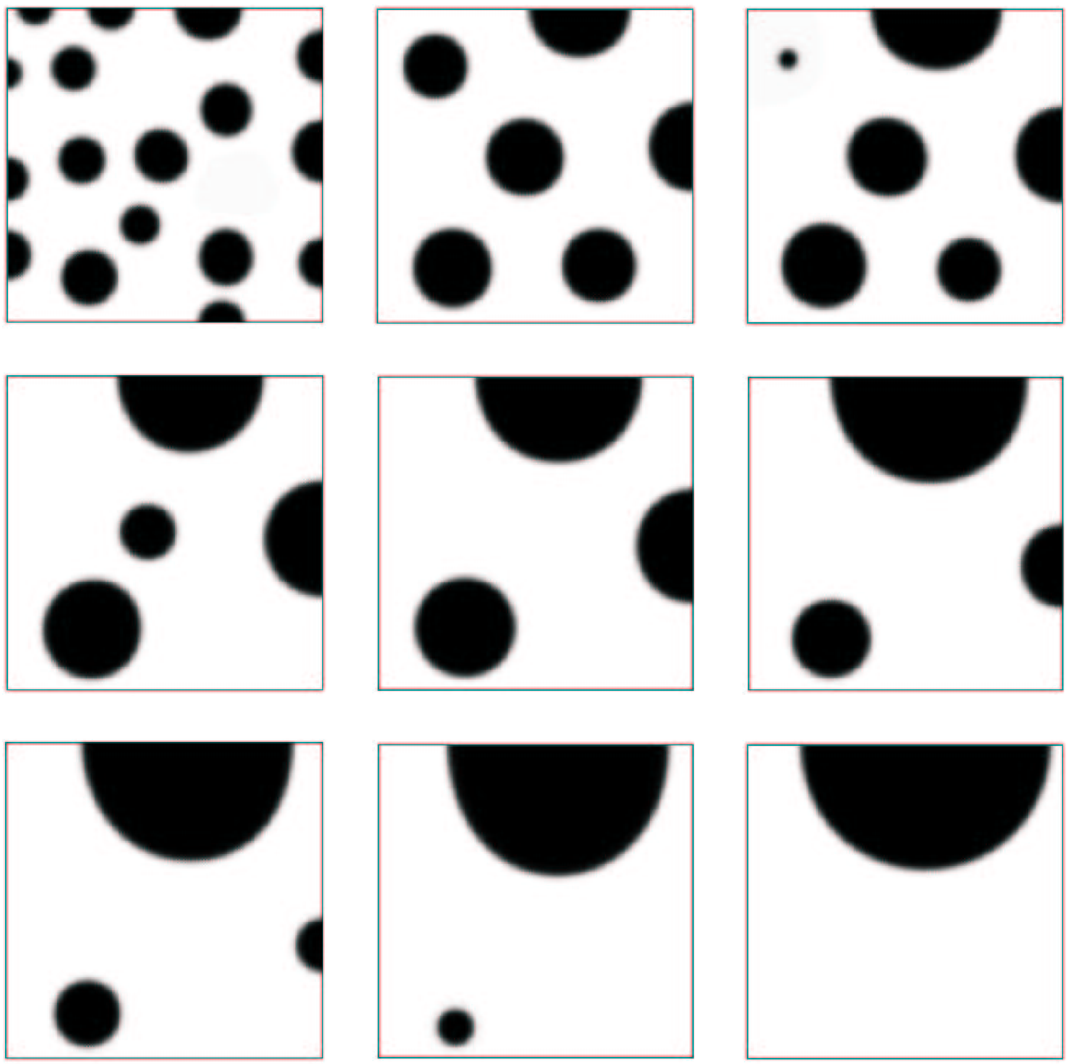

Figure 3.2: $c(\cdot, t)$ plotted for $t = 23.92, 26.31, 31.09, 35.87, 43.05, 50.22, 57.40 \ 62.18$, and 114.79 when $M(c) := 1$.